

Effect of dislocation configuration on non-equilibrium boron segregation during cooling

Huaiyang Cui^{1,2)}, Bing Cao³⁾, and Xinlai He¹⁾

1) Department of Materials Physics, University of Science and Technology Beijing, Beijing 100083, China

2) Department of Applied Physics, Beijing University of Aeronautics and Astronautics, Beijing 100083, China

3) Editorial Department of *J. Univ. Sci. Technol. Beijing*, Beijing 100083, China

(Received 2001-03-27)

Abstract: Different densities and configurations of crystal defects were obtained in an austenitic Fe-30%Ni alloy and an ultra low carbon bainitic (ULCB) alloy by undergoing different deformations and annealing treatments at high temperatures. Boron segregation on grain boundaries and subgrain boundaries during air-cooling were revealed by means of the particle tracking autoradiography technique. It is found that non-equilibrium segregation is resisted in deformed grains after recovery and polygonization, boron-depleted zones seem to be quite clear in recrystallized grains than those in deformed original grains during cooling. Subgrain boundaries and polygonized dislocation cells have a significant effect on non-equilibrium boron segregation during the air-cooling. The results implicate that dislocation configuration is a more important factor affecting boron segregation at grain boundaries rather than the density of defects itself in the grain.

Key words: boron; segregation; recrystallization; dislocation

[This work was financially supported by the National Natural Science Foundation of China (No.59291000).]

Solute atoms can segregate at grain boundaries and affect the properties of materials, and numerous experimental and theoretical works have done on this topic [1-17]. The earlier works have indicated that the segregation of solute atoms on grain boundaries has certain influence on grain boundary migration and phase transformation process [18]. It has been reported by He *et al.* [16] that pre-deformation enhances the degree of non-equilibrium boron segregation at austenitic grain boundaries. Recently, Cui *et al.* [19] investigated the recrystallization of hot deformed materials, and found that the distributions of solute boron atoms have obviously difference between newly recrystallized grains and original deformed grains. Based on this phenomenon, a method of distinguishing the new and old grains in hot-deformed materials was developed [19], but the mechanism of the phenomenon has not been discussed. According to the deformation and recrystallization theory, the density and configuration of crystal defects in deformed matrix will be changed during recovery and recrystallization processes after high temperature deformation. The diffusion of solute atoms from matrix to boundary during segregation will be affected by the interactions of solute atoms with grain boundaries, subgrain boundaries,

vacancies, and dislocation nets, leading to a complicated segregation behavior in deformed materials which has not been defined experimentally.

The aim of this paper is to gain the different densities and configurations of dislocation by distinct heat treatments, and to investigate the effect of crystal defects on non-equilibrium boron segregation during cooling by means of the Particle Tracking Autoradiography (PTA) technique.

1 Experimental

1.1 Materials and test methods

The chemical composition of two alloys investigated is given in **table 1**. The alloys were melted in a vacuum induction furnace, and rolled into plates. Cylindrical specimens, 8 mm in diameter and 12 mm long, were machined out from the plates.

In order to follow static recrystallization of the austenite after high temperature deformation, an interrupted compression test method developed by Petkovic [20] was used in a Gleeble-1500 heat simulator. The procedures of heat treatments used are illustrated in **figure 1**. The softening rate taking place

during the first unloading period at high temperatures can be calculated from the expression

$$X = (\sigma_m - \sigma_r) / (\sigma_m - \sigma_0),$$

where σ_m is the maximum stress before the first unloading, σ_0 and σ_r are the yield stresses during the first and second loading, respectively. An offset strain of 0.2% was used to define the yield stress. The soften-

ing rates for different holding time at 1000°C were evaluated as shown in **figure 2**. The softening consists of two stages: recovery which corresponds to the early stage of softening (usually about 10%), and recrystallization (10%-100%). According to these curves of softening rate to holding time, the degrees of recrystallization are estimated. Further details of this experimental method can be found in reference [20].

Table 1 Chemical composition of the investigated alloys in mass fraction

Alloy	C	Mn	Si	Al	Ti	Nb	B	P	S	N	Ni	Fe
N3	0.01	0.003	0.02	0.210	0.040	0.040	0.0023	0.0078	0.0044	—	29.57	in balance
B1	0.04	1.630	0.46	0.017	0.022	0.052	0.0020	0.0190	0.0020	0.0078	—	in balance

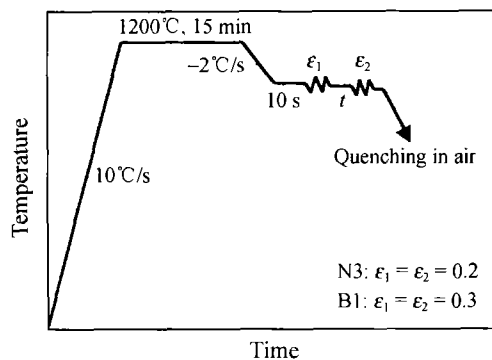


Figure 1 Procedure of interrupted compression tests.

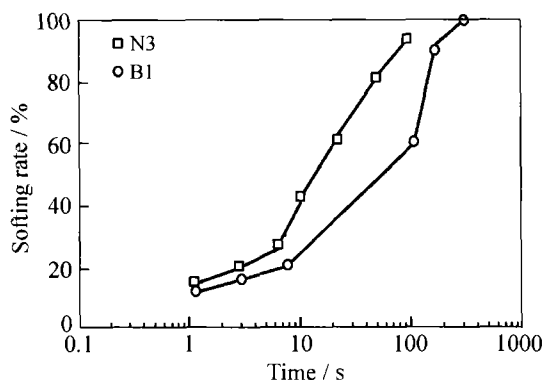


Figure 2 Relationship of softening rate with holding time at 1000°C.

The technique of Particle Tracking Autoradiography (PTA) [21], based on the fission reaction $^{10}\text{B}(n,\alpha)^7\text{Li}$, was applied to reveal the distribution of boron atoms in specimens. In the present work, cellulose acetate films were used as solid detectors and then the film-coated specimens were irradiated to an integrated flux of 5.6×10^{18} neutrons/m², after that the films were etched and examined under an optical microscope.

1.2 Experimental design

In order to study the effect of the amounts and distributions of crystal defects on the non-equilibrium segregation of boron atoms, three treatments, similar to the interrupted compression test procedure in figure

1, were used to gain the midway specimens in the recrystallization process (**figure 3**).

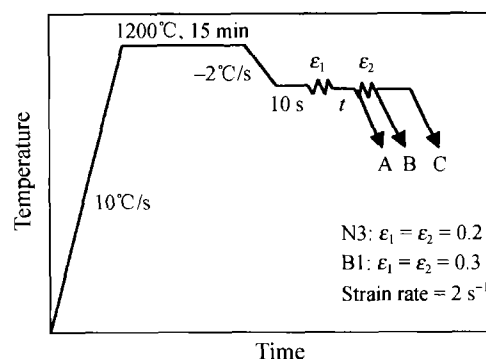


Figure 3 Procedures of treatment.

Treatment A: The specimens were isothermally held at 1200°C for 15 min, then cooled to 1000°C, after deformed, then unloaded and held for an increasing time. During the holding, recovery and recrystallization processes took place, certain newly recrystallized grains formed, the other old deformed matrices were undergoing recovery and polygonization. After the holding, the specimens were quenched in water or cooled in air. The water-quenched specimens kept their boron distribution formed at the isothermal holding, and were regarded as the initial states of the air-cooling. For the air-cooled specimens, boron atoms had enough time to diffuse and form non-equilibrium segregation on grain boundaries during the cooling. This treatment was used to show the difference of segregation processes during the cooling in the new and old grains, which had distinct dislocation densities and configurations.

Treatment B: The specimens were subjected to the first time deformation and isothermal holding, and recrystallization took place in certain area during the holding. Then the specimens were undertaken the second time compression and immediately cooled in air. The second deformation introduced a large amount of deformation in both the newly recrystallized grains

and old original grains. This treatment was designed to examine the difference of non-equilibrium segregation processes in the new and old grains during the air-cooling.

Treatment C: The specimens were undertaken two times compressions, as in treatment B, but after the second deformation, the specimens were annealed for a certain time during which another recovery and polygonization took place in both the new and old grains but no new recrystallization occurred. Following that, the specimens were cooled in air. This treatment was designed to investigate the difference of segregation processes during the cooling between the new and old grains that had suffered the second deformation and recovery.

2 Results

2.1 Boron distributions in the specimens after treatment A

Using treatment A, the Fe-30%Ni alloy held isothermally 7 s after a deformation of 20% at 1000°C, then quenched in water. According to the softening curves shown in figure 2, the specimen just began at that time with recrystallization (about 10%). The boron distribution in this specimen revealed by the

PTA technique is shown in **figure 4** that almost kept the boron distribution before the quenching. But due to the limited cooling rate of the 1500 Gleeble heat simulator, there was weak boron segregation at the grain boundaries, which was of the quenching induced boron segregation [9] and displayed the boundary locations of all original deformed and new grains. It is also observed from figure 4 that the degree of boron segregation on the new grain boundaries (marked A) is stronger than that on the old grain boundaries (marked B), which is an abnormal segregation as a result of grain boundary migration [14,16,22,23] and remained by the quenching. In this case the boron distribution is uniform inside all grains. Instead of the water-quenching, the air-cooling has a lower cooling rate, there is an enough time to allow boron atoms to diffuse to the grain boundaries during the cooling and form non-equilibrium segregation. The boron distributions in the air-cooled specimens after a holding time are revealed by the PTA technique in **figure 5**(a) and (b) for the ultra low carbon bainitic alloy B1 and the Fe-30%Ni alloy N3, respectively. It follows from figure 5 that the stronger boron segregation occurs at the new grain boundaries (A) and the weaker segregation at the old grain boundaries (B).

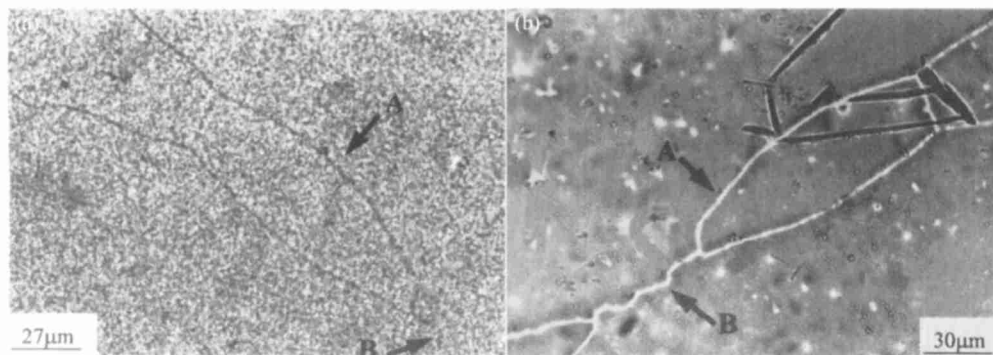


Figure 4 Fe-30%Ni alloy N3, held for 7 s after a deformation of 20% at 1000°C, then quenched in water. (a) boron distribution (PTA picture). (b) an optical micrograph in the same area which has a mirror relation to (a).

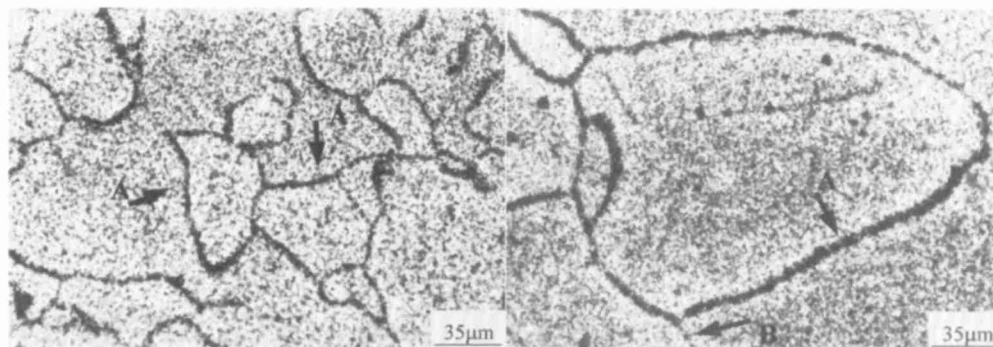


Figure 5 Boron distribution revealed by PTA method. (a) ULCB steel B1, held for 100 s after a deformation of 30% at 1000°C, then cooled in air. (b) alloy N3, held for 7 s after a deformation of 20% at 1000°C, then cooled in air.

Figure 6 shows a low magnification PTA picture of specimen B1 quenched in air after treatment A (corresponding to figure 5(b)). Comparing figures 5 and 6,

another important feature for the air-cooled samples can be observed, boron concentrations in the matrices of the newly recrystallized grains and old deformed

grains are obvious different (on the PTA picture, the densities of etching pits are different in the new and old grains). The new grains seem to be white (the densities of etching pits are lower), where boron atoms are badly depleted. **Figure 7** is another PTA image of an air-cooled sample, shows a large original deformed grain. It can be seen that in the matrix of this deformed grain the density of etching pits is higher, there is boron segregation on the deformation zone (marked A) and the polygonized subgrain boundaries (marked B). TEM examination (**figure 8**) shows that the deformed original grain consists of many dislocation cells (called fine subgrains as well as) with a size of about 1 μm in the Fe-30%Ni alloy after the recovery and recrystallization. It is noted that the fine dislocation cells (**figure 8**) and coarse subgrains (**figure 7**) both consist of dislocation walls (the dislocation densities have some difference). The PTA technique can only reveal bigger subgrain boundaries but fails to reveal fine subgrain (dislocation cell) boundaries due to the limitation of PTA space resolution (about 1-2 μm).

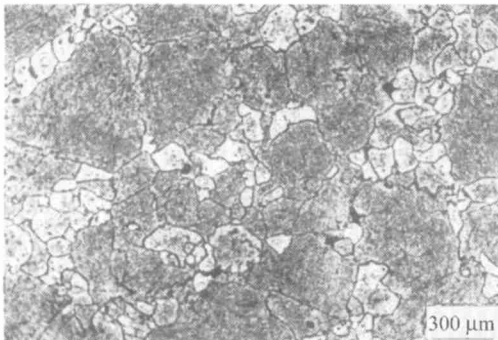


Figure 6 Low magnification morphology corresponding to **figure 5(a)**.

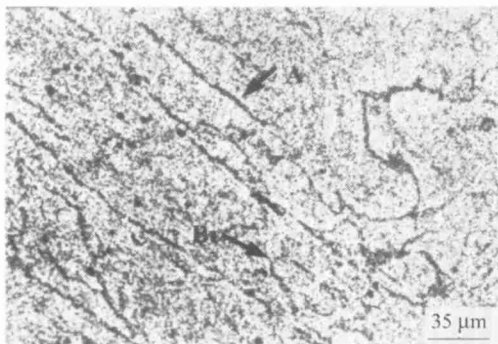


Figure 7 Boron distribution in a large original deformed grain in Fe-30%Ni alloy revealed by PTA. The specimen was held for 3 s after a deformation of 20% at 1000°C, then cooled in air.

2.2 Boron segregation in the air-cooled specimens after the second compression

Using treatment B, the specimens were held 100 s (B1 alloy) and 7 s (N3 alloy) after the first compression, the recovery and recrystallization took place, then compressed again and cooled immediately in air.

The boron segregation was revealed by the PTA technique as shown in **figure 9**. It is found that boron distributions in the new and old grains have difference like that in the specimens without the second compression (treatment A). The new grain boundaries have stronger boron segregation. It seems that the second compression do not affect boron segregation during cooling.



Figure 8 Electron microscopic contrast image of subgrains in Fe-30%Ni alloy. The specimen was held for 3 s after a deformation of 20% at 1000°C, then quenched in water.

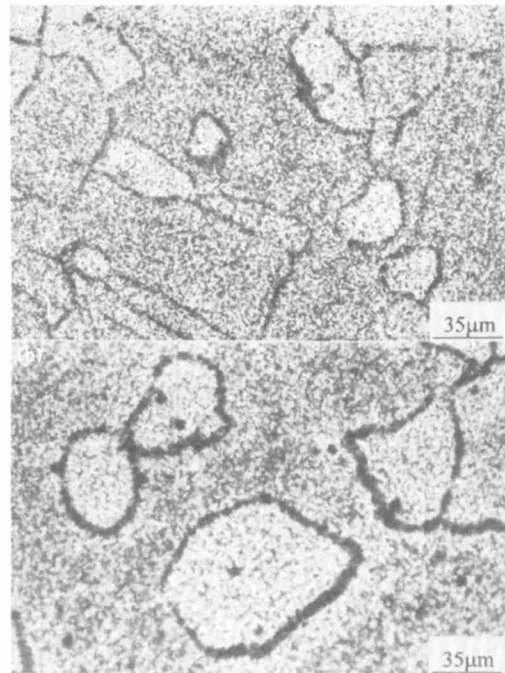


Figure 9 Boron distribution revealed by PTA method. (a) ULCB steel B1, the specimen was held for 300 s after a deformation of 30% again, then immediately cooled in air. (b) Fe-30%Ni alloy N3, the specimen was held for 7 s after a deformation of 20% at 1000°C, deformed 20% again then immediately cooled in air.

2.3 Boron segregation in the air-cooled specimens with annealing for a certain time following the second compression

Using treatment C, the specimens were held 10 s (B1) and 3 s (N3) following the second compression, then cooled in air. The boron segregation was revealed

by the PTA technique in **figure 10**. Microscopic examination indicates that after the second deformation the new recrystallization did not occur during the second annealing time, the new grains growing up during the first annealing became deformed grains and did

not grow again now. It follows from figure 10 that boron segregation takes place at all grain boundaries with the same degree, and the difference of boron distributions in the new and old grains disappears.

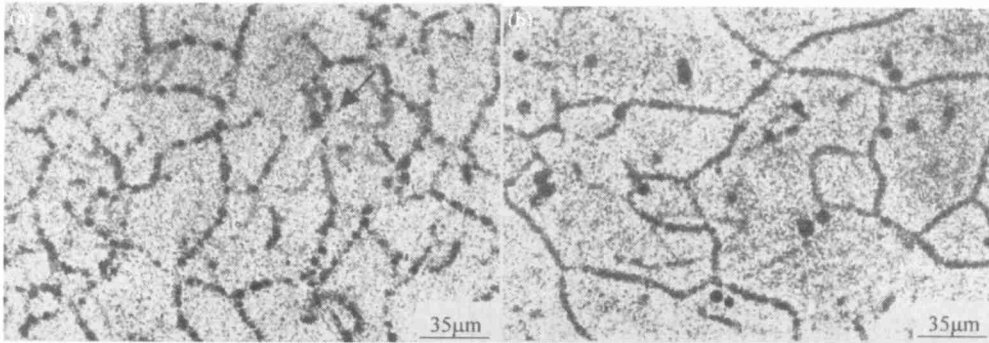


Figure 10 Boron distribution revealed by PTA method. (a) B1 steel, the specimen was held 50 s after a deformation of 30% at 1000°C, deformed 20% again and held for 30 s, then cooled in air. (b) N3 alloy, the specimen was held for 7 s after a deformation of 20% at 1000°C, deformed 20% again and held for 3 s, then cooled in air.

3 Discussion

3.1 Difference of boron concentrations in the new and old grains

Non-equilibrium boron segregation on grain boundaries during the continuous cooling involves the motion of excess vacancy-solute complexes towards the boundaries. Many authors [4-16] have studied systematically this dynamical mechanism. Boron segregations on the boundaries of newly recrystallized grains and old original deformed grains have also been reported [14,16,22], but its mechanism did not be confirmed. In figure 4, the specimen was isothermally held 7 s after the deformation at 1000°C, then quenched in water. During the annealing the recrystallization began, but from figure 4 it is found that boron atoms uniformly distributed in the matrices of all grains except weak boron segregation occurred on the migrating grain boundaries. This picture reflects the real boron distribution after the annealing at the high temperature and indicates that recrystallization could not lead to the difference of boron concentrations in the new grains and old deformed grains. Thus, the difference of boron densities in the new and old grains (figures 5-7) is confirmed to take place during the air-cooling.

The Fe-30%Ni alloy N3 keeps f.c.c. structure in the cooling process, excluding the influence of phase transformation on microstructure and boron distribution. But after the air-cooling the boron distributions in the ultra low carbon bainitic alloy B1 (figure 5) and the Fe-30%Ni alloy (figure 6) had the same characteristics, the similarity of the phenomena indicates that the phase transformation did not change boron dis-

tribution during the air-cooling.

The difference of boron concentrations in the new and old grains is caused by the distinct microstructures of the newly recrystallized grain and the original one, the former has a low dislocation density as a result of recrystallization before the cooling, the later consists of subgrains or polygonized dislocation cells. For example, in a specimen of the Fe-30%Ni alloy which was held for 3 s and quenched in water, TEM shows that its old grain consists of many polygonized dislocation cells, the sizes of the cells were inhomogeneous, and the small one is about 1 µm, as shown in figure 8. Certain deformation bands and bigger subgrains with the size about several microns (or >10 µm) can also be observed in the deformed grains, as shown in figure 7. The PTA technique with a resolution of 1 µm has a limited ability to reveal the subgrain with a size of about several microns, but fails to reveal the subgrains or dislocation cells with the size being estimated to be lower than 1 µm. For the newly recrystallized grains, the dislocation density is lower and the subgrain and cell structure is not clear, so **figure 11** shows a corner of a new grain which has a tangled dislocation cell boundary and just enters into the old deformed grain.

3.2 Boron depleted zones near the new and old grain boundaries in the air-cooled specimen

Figures 5, 6 and 9 show that the boron concentrations (the densities of etching pits) in the newly recrystallized grains are lower than those in the old grains. But if scrutinize, the boron density in the new grain is not uniform, for the large new grains it may be higher at the center of a grain. The boron density in the old original grain is at a higher level, but there is a

narrow boron depleted zone along the grain boundaries. The earlier works [6,11] have pointed out that boron atoms segregated on grain boundaries come from the narrow boron-depleted zone at the two sides of the grain boundaries. It seems that the difference of boron densities in the new and old grains is arisen from the wider boron depleted zones in the new gains and narrow boron depleted zones in the old grains. For small new grains the boron-depleted zones extend to occupy the whole grains and make them to have a bright contrast in the PTA pictures. However, in the old deformed grains, the boron-depleted zone is much narrower, remaining a large number of boron atoms in the matrix. This result conclude that boron atoms diffuse "faster" in the new grains than in the old grains during the air-cooling, the segregation process is somehow resisted in the deformed grains. This will be discussed further in the following part.



Figure 11 TEM contrast image of a new grain in Fe-30%Ni alloy. The specimen was held for 7 s after a deformation of 20% at 1000°C, then quenched in water.

3.3 Effect of dislocation amount and configuration on the boron segregation

Figures 5 and 9 have almost the same characteristics, but the microstructures in the specimens are different. In figure 5, the specimen was annealed for a certain time after the first compression, the newly recrystallized grains have a low dislocation density as a result of recrystallization, while the old original grains consist of many fine subgrain structures as a result of recovery. In figure 9, the second compression introduced large strain or dense dislocations in both the recrystallized grains and the original grains. Comparing with figure 5, in spite of having high strain in all grains in figure 9, the additional dispersed dislocations and excess vacancies do not obviously change the way of the formation of non-equilibrium boron segregation during the cooling.

In treatment C, through a short holding time after the second compression, recovery occurs but recrystallization do not happen in the most grains, in the

matrix the strain reduces, the most dislocations disappear or reconfigure, *i.e.*, polygonization. After the air-cooling, the boron-depleted zones along all grain boundaries are narrow, and the same degree of boron segregation is found in the new and old grains as demonstrated in figure 10. The high dense dislocations introduced by the second compression have evolved into subgrain structures through polygonization (**figure 12**). Thus, all grains have the same microstructure (subgrains inside the grains), and the segregation process is resisted during the air-cooling.

During the non-equilibrium segregation the boron atoms will diffuse to the boundaries (no matter what mechanism, motion of vacancy-solute complexes, or others), and interact with grain boundaries, subgrain boundaries (dislocation walls) and dispersed dislocations. The above experimental results indicate that the boron diffusion in the recrystallized grains is "faster" than that in the polygonized original grains. After the second deformation, although the number of dispersed dislocations increase, which are much more than the number of dislocations in the recovered grains, but they do not affect the boron segregation behavior as shown in figure 9. However after polygonization or recovery again, the dislocations annihilate each other, and the dispersed dislocations reconfigure into the subgrain boundaries or dislocation walls. Evidently, it is this kind of dislocation configuration resisting the segregation. These results imply that dislocation configuration is an important factor affecting non-equilibrium boron segregation, rather than the density of defects itself in the grain.

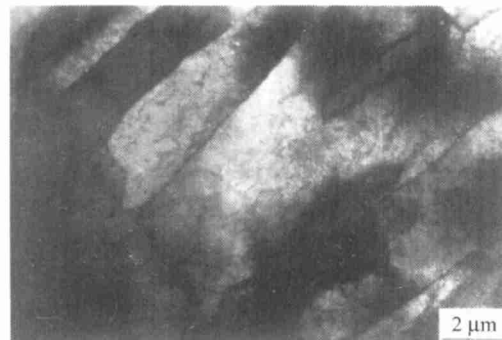


Figure 12 TEM contrast image of subgrains in Fe-30%Ni alloy. The specimen was held for 7 s after a deformation of 20% at 1000°C, deformed 20% again, and annealed for 7 s, then quenched in water.

4 Conclusions

(1) Different densities and configurations of crystal defects were obtained by different treatments of deformations and annealings at high temperatures. Non-equilibrium boron segregations on grain boundaries

and subgrain boundaries during the air-cooling were revealed by the PTA technique.

(2) In the austenite of the Fe-30%Ni alloy and ultra low carbon bainitic alloy, non-equilibrium boron segregation during the cooling is resisted in the deformed original grains after recovery, forming a narrow boron-depleted zone, and the segregation degree decreases.

(3) Boron segregation is enhanced in the newly recrystallized grains with a wide boron-depleted zone leading to a lower boron concentration in small grains

(4) The second compression introduced dense dislocations in both the recrystallized grains and original grains, but this kind of dispersed dislocations seems no influence on boron segregation.

(5) Because of a short time annealing after the second compression making the dispersed dislocations in all deformed grains evolved into the subgrain microstructure, the segregation is resisted. It means that dislocation configuration is an important factor affecting boron segregation, rather than the density of defects itself in the grain.

References

- [1] K.T. Aust, Selective segregation at grain boundaries [J], *Canad. Metall. Quart.*, 13(1974), p.133.
- [2] K.T. Aust, R.E. Hanneman, P. Niessssen, and J.H. Westbrook, Solute-induced hardening near grain boundaries in zone-refined metals [J], *Acta Metall.*, 16(1968), p.291.
- [3] R.G. Faulkner, Non-equilibrium grain-boundary segregation in austenitic alloys [J], *J. Mat. Sci.*, 16(1981), p.373.
- [4] R.G. Faulkner and H. Jiang, Combined model of grain boundary precipitation and segregation of high strength aluminium alloys [J], *Mater. Sci. Technol.*, 9(1993), p.665.
- [5] H. Jiang and R.G. Faulkner, Modeling of grain boundary segregation, precipitation and precipitation-free zones of high strength aluminium alloys [J], *Acta Mater.*, 44(1996), p.1857.
- [6] X.L. He, Y.Y. Chu, and J. Ke, The non-equilibrium segregation of boron to austenite grain boundaries [J], *Acta Metall. Sinica*, 18(1982), p.1.
- [7] T.H. Williams, A.M. Stoneham, and D.R. Harries, The segregation of boron to grain boundaries in solution-treated type 316 austenitic stainless steel [J], *Metall. Sci.*, 10(1976), p.14.
- [8] Y.Y. Chu, X.L. He, L. Tan, T.D. Xu, and J. Ke, Two kinds of boron segregation at austenite grain boundaries [J], *Acta Metall. Sinica*, 23(1987), p.A169.
- [9] X.L. He, Y.Y. Chu, L. Tan, Z.X. Zhou, and J. Ke, The non-equilibrium characteristic of boron segregation at austenite grain boundaries [J], *Acta Metall. Sinica*, 23(1987), p.A291.
- [10] T.D. Xu and S.H. Song, A kinetic model of non-equilibrium grain-boundary segregation [J], *Acta Metall.*, 37(1989), p.2499.
- [11] X.L. He, Y.Y. Chu, and J.J. Jonas, Grain boundary segregation of boron during continuous cooling [J], *Acta Metall.*, 37(1989), p.147.
- [12] X.L. He, Y.Y. Chu and J.J. Jonas, The grain boundary segregation of boron during isothermal holding [J], *Acta Metall.*, 37(1989), p.2905.
- [13] L.T. Mavropoulos, and J.J. Jonas, Effect of the combined addition of niobium and boron on static recrystallization in hot worked austenite [J], *Canad. Metall. Quart.*, 27(1989), p.235.
- [14] S.H. Zhang, X.L. He and T. Ko, Non-equilibrium segregation of solute to grain boundary [J], *J. Metall. Sci.*, 29(1994), p.2633.
- [15] L. Karlsson and H. Norden, Non-equilibrium grain boundary segregation of boron in austenitic stainless steel [J], *Acta Metall.*, 36(1988), p.1.
- [16] X.L. He, M. Djahazi, J.J. Jonas, and J. Jackman, The Non-equilibrium segregation of boron during the recrystallization of Nb-treated HSLA steels [J], *Acta Metall.*, 39(1991), p.2295.
- [17] S.C. Li and S.K. Lui, Multicomponent segregation along boundary and thermodynamical analysis of Fe-C-Si-Mn alloy [J], *Acta Metall. Sinica*, 27(1991), p.B161.
- [18] M.B. Kasen, Solute segregation and boundary structural change during grain growth [J], *Acta Metall.*, 31(1983), p.489.
- [19] H.Y. Cui, X.L. He and J. Ke, Study of recrystallization of boron-treated ultra low carbon bainitic steel by PTA technique [J], *J. Iron Steel Research*, 7(1995), p.58.
- [20] R.A. Petkovic, M.L. Luton, and J.J. Jonas, Recovery and recrystallization of polycrystalline copper after hot working [J], *Acta Metall.*, 27(1979), p.1633.
- [21] X.L. He and Y.Y. Chu, The application of $^{10}\text{B}(n,\alpha)^7\text{Li}$ fission reaction to study boron behaviour in materials [J], *J. Phys. D: Appl. Phys.*, 16(1983), p.1145.
- [22] H.Y. Cui and X.L. He, Boron segregation on grain boundary during recrystallization, [in] *THERMEC'97* [C], Australia, 1997, p.363.
- [23] P. Wu and X.L. He, Grain boundary non-equilibrium segregation: retrospect/prospect [J], *Acta Metall. Sinica*, 35(1999), p.1009.